Communication

Pip-HoGu, an artificial assembly with cooperative DNA recognition capable of mimicking transcription factor pairs

Zutao Yu, Chuanxin Guo, Yulei Wei, Kaori Hashiya, Toshikazu Bando, and Hiroshi Sugiyama

J. Am. Chem. Soc., **Just Accepted Manuscript** • DOI: 10.1021/jacs.7b13275 • Publication Date (Web): 02 Feb 2018

Pip-HoGu, an artificial assembly with cooperative DNA recognition capable of mimicking transcription factor pairs

Zutao Yu†, Chuanxin Guo†, Yulei Wei†, Kaori Hashiya†, Toshikazu Bando†, Hiroshi Sugiyama*†‡

† Department of Chemistry, Graduate School of Science and ‡Institute for Integrated Cell-Material Sciences (iCeMS), Kyoto University, Kitashirakawa-Oiwakecho, Sakyo-ku, Kyoto 606-8502, Japan

Supporting Information Placeholder

ABSTRACT: Cooperation between pairs of transcription factors (TFs) has been widely demonstrated to play a pivotal role in the spatiotemporal regulation of gene expression, but blocking cooperative TF pair–DNA interactions synergistically has been challenging. To achieve this, we designed programmable DNA binder pyrrole-imidazole polyamides conjugated to host–guest assemblies (**Pip-HoGu**) to mimic the cooperation between natural TF pairs. By incorporating cyclodextrin (Cyd)–adamantane (Ada), we synthesized **Ada1** (PIP1-Ada) and **Cyd1** (PIP2-Cyd), which were evaluated using T_m, EMSA, competitive, and SPR assays and molecular dynamics studies. The results consistently demonstrated that **Pip-HoGu** system formed stable noncovalent cooperative complexes, thereby meeting key criteria for mimicking a TF pair. The system also had a longer recognition sequence (two-PIP binding length plus gap distance), favorable sequence selectivity, higher binding affinity, and in particular, a flexible gap distance (0–5 bp). For example, **Ada1**–**Cyd1** showed thermal stability of 7.2 °C and a minimum free energy of interaction of –2.32 kcal·mol^{-1} with a targeting length of 14 bp. Furthermore, cell-based evaluation validated the capability of **Pip-HoGu** to exhibit potent cooperative inhibitory effects on gene expression under physiological conditions by disrupting TF pair–DNA function. In conclusion, the modular design of **Pip-HoGu** defines a general framework for mimicking naturally occurring cooperative TF pair–DNA interactions that offers a promising strategy for applications in the precise manipulation of cell fate.

Manipulating spatiotemporally variable gene expression has been the goal of generations of scientists[1,2]. In mammals, there are approximately 1000 transcription factors (TFs) that extensively regulate gene expression patterns, and 55–70% of these TFs may be functioning as cooperative TF pairs via homo-/heterodimers to ensure high binding affinity and extended recognition sequence[3,4]. Programmable molecules, e.g., nucleic acid analogues and pyrrole-imidazole polyamides (PIPs), can disrupt individual TF–DNA interactions[5-7], but cannot block interactions between collaborative TF pairs and DNA. More specifically, the gap sequences between the two binding motifs of the TF pair are not conserved and the gap distances are relatively flexible, ranging from –1–5 bp[8]. Most significantly, by switching cooperative partners, TF pairs can exert divergent biological functions. For example, Sox2/Oct4 instigates pluripotent gene activation, but Oct4/Sox17 functions as a HEX activator and Sox2/Pax6 plays a pivotal role in ocular lens development[9,10]. Accordingly, disrupting the individual binding sites of Sox2 or Oct4, rather than synergistically disrupting those of both TFs will result in complex biological outcomes. Therefore, novel strategies are needed to address these challenges to the implementation of deliberate and precise manipulation of gene expression patterns.

PIPs are the best characterized programmable DNA minor-groove binders that can compete with TF binding, with the binding rules that Py/Im recognizes C/G, Im/Py recognizes G/C, and Py/Py recognizes A/T and T/A[11]. Despite substantial progress, there is still a long way to go before these molecules can be applied clinically[7,12]. The short recognition sequences of PIPs lead to high off-target rates, but the extension of PIP length significantly impairs its cell permeability[13,14]. Critically, the fixed PIPs-binding motif (4–8 bp) without elasticity, is unsuitable for blocking flexible TF binding, especially that of TF pairs[15].

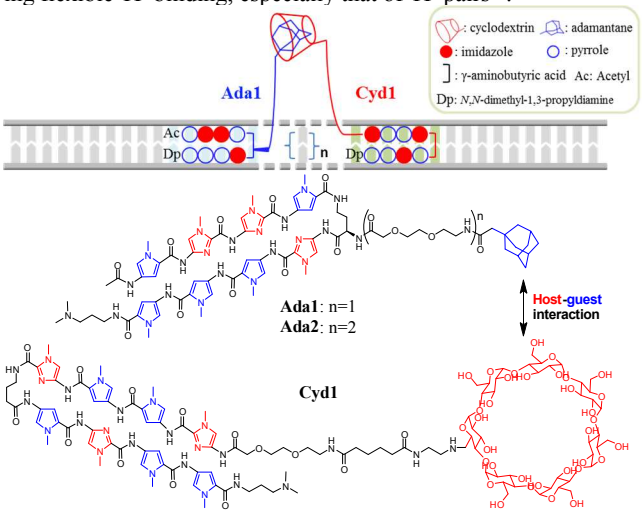

Figure 1. Overview of cooperative interactions of a TF pair targeting a sequence associated with two components of **Pip-HoGu** assembly, **Ada1** and **Cyd1**. n = gap distance. (Bottom) Chemical structures of **Ada1**, **Ada2**, and **Cyd1**.

In this context, we envisaged the integration of PIPs with a cooperative system to mimic the homo- or heterodimer binding systems of TF pairs. There are several classic noncovalent cooperative systems, including nucleic acid analogues, metal ion–ligand, and host–guest systems (e.g., cyclodextrin (Cyd), cucurbit[n]uril, and carcerands with guests)[16-21]. Among these cooperative systems, Cyd–adamantane (Ada) has been extensively studied as an exemplary host–guest system both in vitro and in cells[22,23]. By replacing a leucine-zipper dimerization domain with Cyd/Ada, Morii and colleagues designed an artificial system in which the cooperative Cyd–Ada interaction highly stabilized the interaction

of DNA with the DNA-binding domains of GCN4 homodimer[24,25]. The work of Mascarenas and colleagues of Cyd–Ada assisted DNA-binding peptide–distamycin derivatives represented a step forward in the development of smaller, selective, and ligand-responsive systems[26]. Accordingly, the design of programmable DNA binder/host–guest scaffold for mimicking cooperative TF-pair systems and especially their cell-based applications is highly attractive.

To achieve this, we designed PIPs conjugated to a host–guest Cyd–Ada scaffold, i.e., **Pip-HoGu**. We first evaluated them in vitro using the DNA-binding sequences of the Tax/CREB heterodimer, which functions by cooperative recruitment of p300 that is essential for HLTV-1 virus amplification[27,28] **Ada1** (PIP1-Ada) consists of a PIP moiety to target the Tax binding site (5′-WWGGCW-3′) conjugated to Ada via a mini-PEG linker (Figure 1)[24]. Host conjugate **Cyd1** (PIP2-Cyd) contains a Cyd moiety and a CREB-competitive-binding PIP (5′-WGWCGW-3′). We generated series of positive- and negative-binding sequences, and the difference in binding originates from the relative positions of the **Ada1** and **Cyd1** binding sites (Figure 2A). In positive-binding sequences, Cyd–Ada covers only a short distance (equal to the gap distance) (Figure S1). In contrast, in the negative-binding mode, Ada must bridge two PIP-binding sites plus the gap distance, making it impossible for Ada to interact with Cyd.

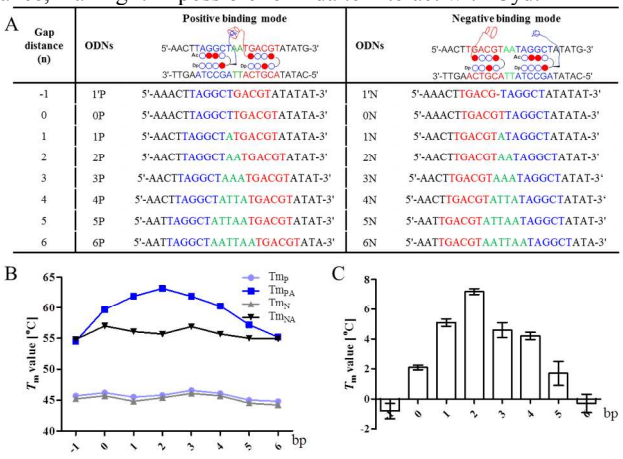

Figure 2. T_m assay illustrating the cooperativity of **Pip-HoGu**. (A) The DNA oligomers (ODNs) used in the T_m assay, including positive (ODN1′P–ODN6P) and negative (ODN1′N–ODN6N) binding sequences. The gap distance (green) is the number of bp between the binding sites of **Ada1** (blue) and **Cyd1** (red). The chart only shows the forward DNA strand. (B) T_m profiles of positive ODNs (T_{mP}, light blue), negative ODNs (T_{mN}, gray), positive ODNs/**Ada1–Cyd1** (T_{mPA}, blue), and negative ODNs/**Ada1–Cyd1** (T_{mNA}, black). (C) $\Delta\Delta T_m$ profiles of cooperativity of **Ada1–Cyd1** assemblies. $\Delta T_m = T_m$ (ODNs/PIPs) – T_m (ODNs); $\Delta\Delta T_m = \Delta T_{mP} - \Delta T_{mN}$. Error bars indicate the standard deviation of three replicates.

A thermal stabilization assay (T_m assay) was performed to evaluate the cooperative binding potency and how it was influenced by the gap distance[29]. In the positive-binding mode, the overall thermal stability of **Ada1–Cyd1** had a ΔT_{mP} value of 9–15 °C ($\Delta T_{mP} = T_{mP} - T_m$) in a gap-distance-dependent manner (Figure 2B, Table S1). In negative-binding mode, however, there were no gap-distance-dependent effects on the thermal stability of **Ada1–Cyd1** with ΔT_{mN} values around 9–10 °C (Table S1). In the control experiment with mixture of PIP1 and PIP2, there was no significant difference of thermal stability between positive- and negative-binding sequences (Figure S2). Therefore, the discrepancy of thermal stabilization effect between positive- and negative-binding modes should mainly attributable to the cooperative interaction of the Cyd–Ada complexes[30,31]. The results showed that positive-binding ODNs with 0–5 bp gap distances displayed cooperative binding function, and no cooperative effect was observed with gap distances ≥6 bp (Figure 2C). These results highlight the gap-distance dependency of cooperative binding energies. ODN2P with a 2-bp gap distance demonstrated the highest level of cooperation ($\Delta\Delta T_m$ = 7.2 °C). Of note, a 1-bp mismatch T_m assay showed that **Pip-HoGu** exhibited high sequence specificity with a $\Delta\Delta T_m$ of 8.3 °C (Table S2)[32].

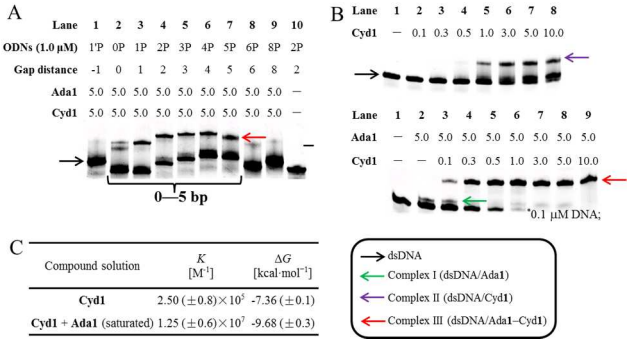

Figure 3. EMSA illustrating the cooperativity of **Pip-HoGu**. (A) The gel-shift behavior of all the positive-binding sequences with **Ada1–Cyd1**. Concentrations are shown in figure. (B) Quantitative EMSA of ODN2P with **Cyd1** at various concentrations (top) and **Cyd1** supplemented with saturated **Ada1** (bottom). ODNs concentration: 0.1 μM. (C) Equilibrium association constants and free energies for ODN2P with **Ada1–Cyd1**.

Parallel to the T_m assay, electrophoretic mobility shift assays (EMSAs) were conducted to visualize band-shift behavior upon formation of stable complexes[33]. The band upshifts for **Ada1**, **Cyd1**, and **Ada1–Cyd1** with ODN2P can be clearly distinguished (Figure S3). Next, fixed concentrations of **Ada1–Cyd1** were allowed to equilibrate with all ODNs. In agreement with the results of the T_m assay, the appearance of an upshifted band showed that ODNs with positive-binding mode and 0–5 bp gap distances display cooperative binding (Figure 3A). **Ada1–Cyd1** shows substantially weaker band shift with ODN0P, for which steric hindrance might be partially responsible. In comparison, no complexes were observed for DNA sequences of –1 bp and >6 bp. Moreover, no negative-binding mode DNA sequences could form upshifted band indicative of cooperative complexes, and there was also no upshifted band of negative ODNs with **Ada1** or **Cyd1** individually, suggesting cooperative complex mediated sequence selectivity (Figure S4)[3]. In addition, competitive EMSA assays showed that cooperation was weakened in the presence of a guest competitor (Figure S5)[34].

Quantitative EMSAs were performed to analyze the magnitude of cooperativity and the equilibrium association constant was determined by fitting to the Langmuir binding isotherm[35]. The increase in the upshifted band for ODN2P at various concentrations of **Cyd1** alone and in the presence of **Ada1** at excess concentration demonstrates the cooperative effect (Figure 3B)[36]. Specifically, the data generated an equilibrium association constant of 2.50×10^5 M^{-1} (K_1) for **Cyd1** alone, and promisingly increased to 1.25×10^7 M^{-1} ($K_{1,2}$) in the presence of **Ada1** (Figure 3C). Using the equation for the free energy of binding, the free energies of binding for **Cyd1** alone and in the presence of **Ada1** were –7.36 and –9.68 kcal·mol^{-1}, respectively, giving a minimum free energy of interaction ($G_{2\text{-}1} - G_2$) of –2.32 kcal·mol^{-1}[37]. Therefore, **Pip-HoGu** has superior cooperation-stabilization effects to the previously reported 8-bp DNA duplex (–2.2 kcal·mol^{-1}) and the natural phage λ repressor system (–2.0 kcal·mol^{-1}).[37,38]. Concomitantly, a surface plasmon resonance (SPR) assay was further validated quantitatively the cooperative effects of **Pip-HoGu** assembly (Table S3, Figure S7)[39].

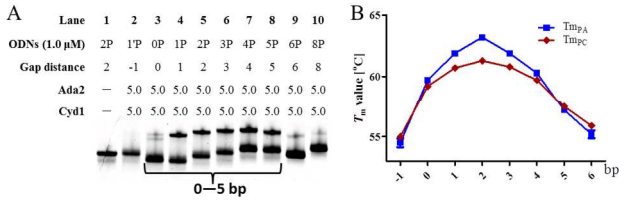

Figure 4. Mechanistic studies of cooperative binding. (A) Gel-shift behavior **Ada2–Cyd1**. (B) T_m profiles of all positive-binding sequences in the presence of **Ada1–Cyd1** (T_{mPA}, blue, same as Figure 2B) and **Ada2–Cyd1** (T_{mPB}, red).

Continually, we studied the influence of linker length on cooperative binding since the underlying mechanisms of gap-distance-dependent cooperativity (≤5 bp) are not totally clear[19]. For this, we used **Ada2**, which has a long, double mini-PEG linker (Figure 1). In the EMSA and T_m assay, **Ada2–Cyd1** showed similar cooperative patterns to **Ada1–Cyd1**, i.e., only those DNA sequences with gap distances of 0–5 bp could form cooperative complexes (Figure 4A, B). Specifically, **Ada2–Cyd1** showed lower stability for gap distances of 0–4 bp in the T_m assay. This demonstrated that an extra-long linker might destabilize the binding affinity of the complex over short gap distances. Interestingly, when the gap distance was extended to 5–6 bp, **Ada2–Cyd1** displayed slightly higher stability than **Ada1–Cyd1** because the longer and more flexible linker can reduce the tension of complex formation. In conclusion, the cooperative energy of **Pip-HoGu** was highly distance dependent and that gap distances of >5 bp diminish the cooperation, even when the linker region was long enough to allow the encounter of host–guest moieties. This can be explained by the hydrophobic and van der Waals interactions of Cyd–Ada[16,40].

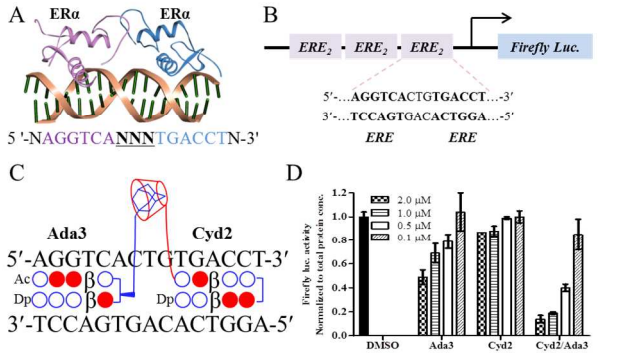

Figure 5. Cell-based assay of **Pip-HoGu**. (A) Crystal structure of ERα homodimer and DNA sequence. (B) Schematic diagram of ERE-driven luciferase in T47DK-BLuc cells. (C) The structural design of **Ada3** and **Cyd2** targeting ERE sites (Figure S8). (D) Luciferase activity assay after normalization to the total protein concentration.

Because we had compellingly demonstrated its cooperativity in several in vitro assay systems, we were encouraged to apply **Pip-HoGu** to a cell-based assay. The estrogen response element (ERE) is the specific target motif of the estrogen receptor α (ERα) homodimer, which induces significant downstream gene activation (Figure 5A)[41]. In ERα-positive, 17β-estradiol-stimulated T47D-KBluc cells that highly express luciferase after binding of three tandem ERα TF pairs, **Ada3**, **Cyd2**, and **Ada3–Cyd2** that bound to the ERE consensus half-site (5′-WGGWCW-3′) were tested for 48 h together with the delivery reagent endoporter (Figure 5B, C)[42]. The effects of PIPs were measured by luciferase activity normalized to total protein concentration[43,44]. Monotreatment with **Ada3** showed only moderate-to-weak inhibitory activity ($IC_{50} \geq 2$ μM) while very weak activity was observed for **Cyd2** (<20% inhibition) (Figure 5D). When cells were treated with a combination of **Ada3** and **Cyd2**, 4–5-fold enhancement of the inhibitory effect was observed, which strongly correlated with the cooperative interactions of the host–guest system. The use of endoporter ensured that **Ada3** and **Cyd2** reached homodimer-binding sites at the same time, and it is plausible that **Pip-HoGu** could also work well for heterodimer binding sites in the absence of endoporter[44]. This cell-based assay system demonstrated for the first time that the individual host–guest interactions of **Pip-HoGu** could effectively stabilize the PIP pair–DNA cooperative interaction and potently inhibit natural TF-pair binding in cells.

Cooperation between TF pairs is ubiquitous in cells[8]. Our prototype **Pip-HoGu** defines a general framework for mimicking cooperative TF pair–DNA interactions through the integration of programmable DNA binders and a host–guest system. In vitro assays showed that **Ada1–Cyd1** assemblies formed stable cooperative binding complexes with target DNA sequences with 0–5 bp gap distances. In essence, the cell-based assay demonstrated that our artificial **Ada3–Cyd2** assemblies formed highly stable cooperative complexes that competed with naturally occurring cooperative TF pair–DNA systems. Therefore, **Pip-HoGu** could be applied to the regulation of spatiotemporally variable gene expression patterns.

ASSOCIATED CONTENT

Supporting Information

Experimental details including synthesis, evaluation method and supporting data. This material is available free of charge via the Internet at http://pubs.acs.org.

AUTHOR INFORMATION

Corresponding Author

*hs@kuchem.kyoto-u.ac.jp

Notes

The authors declare no competing financial interests.

ACKNOWLEDGMENT

This work was supported by JSPS KAKENHI Grant NO. JP16H06356, "Basic Science and Platform Technology Program for Innovative Biological Medicine by Japan Agency for Medical Research and Development (AMED)" , and "the Platform Project for Supporting Drug Discovery and Life Science Research funded by AMED". We thank China Scholarship Council support Z. Y.

REFERENCES

(1) Takahashi, K.; Yamanaka, S. *Cell* **2006**, *126*, 663-676.
(2) Srivastava, D.; DeWitt, N. *Cell* **2016**, *166*, 1386-1396.
(3) Morgunova, E.; Taipale, J. *Curr. Opin. Struct. Biol.* **2017**, *47*, 1-8.
(4) Stampfel, G.; Kazmar, T.; Frank, O.; Wienerroither, S.; Reiter, F.; Stark, A. *Nature* **2015**, *528*, 147-151.
(5) Gottesfeld, J. M.; Neely, L.; Trauger, J. W.; Baird, E. E.; Dervan, P. B. *Nature* **1997**, *387*, 202-205.
(6) Dragulescu-Andrasi, A.; Rapireddy, S.; He, G.; Bhattacharya, B.; Hyldig-Nielsen, J. J.; Zon, G.; Ly, D. H. *J. Am. Chem. Soc.* **2006**, *128*, 16104-16112.
(7) Taniguchi, J.; Pandian, G. N.; Hidaka, T.; Hashiya, K.; Bando, T.; Kim, K. K.; Sugiyama, H. *Nucleic Acids Res.* **2017**, *45*, 9219-9228.
(8) Jolma, A.; Yin, Y.; Nitta, K. R.; Dave, K.; Popov, A.; Taipale, M.; Enge, M.; Kivioja, T.; Morgunova, E.; Taipale, J. *Nature* **2015**, *527*, 384-388.
(9) Aksoy, I.; Jauch, R.; Chen, J.; Dyla, M.; Divakar, U.; Bogu, G. K.; Teo, R.; Leng Ng, C. K.; Herath, W.; Lili, S.;

Hutchins, A. P.; Robson, P.; Kolatkar, P. R.; Stanton, L. W. *EMBO J.* **2013**, *32*, 938-953.

(10) Kamachi, Y.; Uchikawa, M.; Tanouchi, A.; Sekido, R.; Kondoh, H. *Genes Dev.* **2001**, *15*, 1272-1286.

(11) Trauger, J. W.; Baird, E. E.; Dervan, P. B. *Nature* **1996**, *382*, 559-561.

(12) Kurmis, A. A.; Yang, F.; Welch, T. R.; Nickols, N. G.; Dervan, P. B. *Cancer Res.* **2017**, *77*, 2207-2212.

(13) Edelson, B. S.; Best, T. P.; Olenyuk, B.; Nickols, N. G.; Doss, R. M.; Foister, S.; Heckel, A.; Dervan, P. B. *Nucleic Acids Res.* **2004**, *32*, 2802-2818.

(14) Kawamoto, Y.; Sasaki, A.; Chandran, A.; Hashiya, K.; Ide, S.; Bando, T.; Maeshima, K.; Sugiyama, H. *J. Am. Chem. Soc.* **2016**, *138*, 14100-14107.

(15) Deplancke, B.; Alpern, D.; Gardeux, V. *Cell* **2016**, *166*, 538-554.

(16) Yu, G.; Jie, K.; Huang, F. *Chem. Rev.* **2015**, *115*, 7240-7303.

(17) Rodriguez, J.; Mosquera, J.; Garcia-Fandino, R.; Vazquez, M. E.; Mascarenas, J. L. *Chem. Sci.* **2016**, *7*, 3298-3303.

(18) Azuma, Y.; Imanishi, M.; Yoshimura, T.; Kawabata, T.; Futaki, S. *Angew. Chem. Int. Ed. Engl.* **2009**, *121*, 6985-6988.

(19) Ihara, T.; Uemura, A.; Futamura, A.; Shimizu, M.; Baba, N.; Nishizawa, S.; Teramae, N.; Jyo, A. *J. Am. Chem. Soc.* **2009**, *131*, 1386-1387.

(20) Machida, T.; Novoa, A.; Gillon, É.; Zheng, S.; Claudinon, J.; Eierhoff, T.; Imberty, A.; Römer, W.; Winssinger, N. *Angew. Chem. Int. Ed. Engl.* **2017**, *56*, 6762-6766.

(21) Zhou, X.; Su, X.; Pathak, P.; Vik, R.; Vinciguerra, B.; Isaacs, L.; Jayawickramarajah, J. *J. Am. Chem. Soc.* **2017**, *139*, 13916-13921.

(22) Morii, T.; Tanaka, T.; Sato, S.-i.; Hagihara, M.; Aizawa, Y.; Makino, K. *J. Am. Chem. Soc.* **2002**, *124*, 180-181.

(23) Lai, J.; Shah, B. P.; Garfunkel, E.; Lee, K.-B. *ACS Nano* **2013**, *7*, 2741-2750.

(24) Ueno, M.; Murakami, A.; Makino, K.; Morii, T. *J. Am. Chem. Soc.* **1993**, *115*, 12575-12576.

(25) Aizawa, Y.; Sugiura, Y.; Ueno, M.; Mori, Y.; Imoto, K.; Makino, K.; Morii, T. *Biochemistry* **1999**, *38*, 4008-4017.

(26) Blanco, J. B.; Dodero, V. I.; Vázquez, M. E.; Mosquera, M.; Castedo, L.; Mascareñas, J. L. *Angew. Chem. Int. Ed. Engl.* **2006**, *45*, 8210-8214.

(27) Livengood, J. A.; Fechter, E. J.; Dervan, P. B.; Nyborg, J. K. *Front. Biosci.* **2004**, *9*, 3058-3067.

(28) Matsuoka, M.; Jeang, K.-T. *Nat. Rev. Cancer.* **2007**, *7*, 270-280.

(29) Guo, C.; Kawamoto, Y.; Asamitsu, S.; Sawatani, Y.; Hashiya, K.; Bando, T.; Sugiyama, H. *Bioorg. Med. Chem.* **2015**, *23*, 855-860.

(30) Ihara, T.; Takeda, Y.; Jyo, A. *J. Am. Chem. Soc.* **2001**, *123*, 1772-1773.

(31) Panjkovich, A.; Melo, F. *Bioinformatics* **2005**, *21*, 711-722.

(32) Yu, Z.; Taniguchi, J.; Wei, Y.; Pandian, G. N.; Hashiya, K.; Bando, T.; Sugiyama, H. *Eur. J. Med. Chem.* **2017**, *138*, 320-327.

(33) Kameshima, W.; Ishizuka, T.; Minoshima, M.; Yamamoto, M.; Sugiyama, H.; Xu, Y.; Komiyama, M. *Angew. Chem. Int. Ed. Engl.* **2013**, *52*, 13681-13684.

(34) Hossain, M. A.; Hamasaki, K.; Takahashi, K.; Mihara, H.; Ueno, A. *J. Am. Chem. Soc.* **2001**, *123*, 7435-7436.

(35) Heddi, B.; Cheong, V. V.; Martadinata, H.; Phan, A. T. *Proc. Natl. Acad. Sci. U.S.A.* **2015**, *112*, 9608-9613.

(36) Sánchez, M. I.; Mosquera, J.; Vázquez, M. E.; Mascareñas, J. L. *Angew. Chem. Int. Ed. Engl.* **2014**, *53*, 9917-9921.

(37) Distefano, M. D.; Dervan, P. B. *Proc. Natl. Acad. Sci. U.S.A.* **1993**, *90*, 1179-1183.

(38) Ackers, G. K.; Johnson, A. D.; Shea, M. A. *Proc. Natl. Acad. Sci. U.S.A.* **1982**, *79*, 1129-1133.

(39) Asamitsu, S.; Li, Y.; Bando, T.; Sugiyama, H. *Chembiochem* **2016**, *17*, 1317-1322.

(40) Harada, A.; Takashima, Y.; Nakahata, M. *Acc. Chem. Res.* **2014**, *47*, 2128-2140.

(41) Boyer, M.; Poujol, N.; Margeat, E.; Royer, C. A. *Nucleic acids research* **2000**, *28*, 2494-2502.

(42) Wilson, V. S.; Bobseine, K.; Gray, J. L. E. *Toxicological Sciences* **2004**, *81*, 69-77.

(43) Nickols, N. G.; Szablowski, J. O.; Hargrove, A. E.; Li, B. C.; Raskatov, J. A.; Dervan, P. B. *Mol. Cancer Ther.* **2013**, *12*, 675-684.

(44) Summerton, J. E. *Annals of the New York Academy of Sciences* **2005**, *1058*, 62-75.

Table of Content (TOC) graphic: